https://doi.org/10.5194/egusphere-2026-2821
Preprint. Discussion started: 6 July 2026

On transient thermally induced stability changes in high-mountain permafrost rock walls: A semiquantitative modeling approach applied to recent landslides at Rasac (Cordillera Huayhuash, Peru, 2023) and Blatten (Swiss Alps, 2025)

Wilfried Haeberli[1], Denis Cohen[2], Lukas U. Arenson[3]

[1]Geography Department, University of Zurich, 8047 Zurich, Switzerland
[2]CoSci LLC, 54519 Conover, WI, USA
[3]BGC Engineering Inc., V6Z 0C8Vancouver BC, Canada

Correspondence to: Wilfried Haeberli (wilfried.haeberli@geo.uzh.ch)

Abstract. Climate-induced warming affects physical, mechanical and hydraulic properties of permafrost rock walls in cold mountain regions. While detailed understanding of the complex interaction between rock structures, ice and water remains challenging, the overall effect of thermally induced stability reduction seems evident and best explains the recent increase in the number of large rock-ice avalanches. Time-dependent modeling of thermal conditions in the pre-event failure zone of two recent events at Rasac ridge (2023) in the Cordillera Huayhuash, Peru, and at Blatten (2025) in the Swiss Alps documents marked subsurface warming during the past about 150 years down to about 100 meters or more together with a remarkable inertia of the associated temperature change. Both investigated mass movements must have detached from quite cold permafrost with permafrost depths in places exceeding 200 to 300 meters but with pronounced asymmetric thermal conditions as is characteristic for sharp mountain ridges. In the Blatten case, increasing water infiltration from the warmer sunny side may have contributed to the release of an already weak slope which must have developed subcritical rock-mechanical conditions over much longer time.

The large amount of heat already now stored deep below the surface constitutes a strong long-term commitment concerning the future stability of permafrost rock slopes. Ongoing atmospheric and subsurface temperature rise are likely to further enhance related stability reductions. Hazard and risk assessments concerning cold mountains must adequately consider such strongly time-dependent aspects.

1 Introduction

Stability assessments concerning steep, ice-clad mountain slopes must essentially consider three basic factors: Topography, geology and water, while for water the difference between its frozen and unfrozen state is of uppermost relevance. Under conditions of global warming, by far the strongest and fastest change presently concerns the ice component and how its change influences water flow, pressures and strength within these rock masses.

https://doi.org/10.5194/egusphere-2026-2821
Preprint. Discussion started: 6 July 2026

As atmospheric temperatures rise, mountains inevitably also experience an increase in temperature. Where these mountains are frozen throughout the year (permafrost), such warming affects their stability, including rockfall activity (Haeberli et al., 1997; Davies et al., 2001; Gruber and Haeberli, 2007; Harris et al., 2009; Krautblatter et al., 2012, 2013; Krautblatter and Draebing, 2014; Krautblatter and Leith, 2015; Kenner et al., 2022; Etzelmüller et al., 2023; Hartmeyer and Otto, 2024; Stoffel et al., 2024; Fey et al., 2025; Yang et al., 2026; Magnin et al., 2026). The primary physical process thereby includes a combination of

(1) deep warming (characteristic depth range tens of meters: Etzelmüller et al., 2020; Noetzli et al., 2024; Kenner et al., 2024) of frozen rocks, the strength and stability of which are heavily temperature-dependent (Davies et al., 2001; Krautblatter et al., 2013; Mamot et al., 2018, 2021);
(2) slow thawing of frozen rocks at the permafrost table (depth range meters) eliminating ice fillings, thereby drastically reducing cohesion and, together with increasing hydraulic permeability, reducing effective stresses as pore water pressures can build up;
(3) increasing water content in frozen parts within frozen rocks, especially at temperatures near 0°C ("warm permafrost"); and
(4) onset of water circulation along open cracks and fissures, thereby percolating into permafrost and accelerating heat exchange at depth through advection (Weber et al., 2025) and building up high local water pressure (Offer et al., 2025).

While process 4 largely escapes direct measurements in the field for logistic (access) reasons, processes 1, 2 and 3 are systematically observed within the framework of global permafrost monitoring via borehole temperatures, repeated resistivity soundings (Hilbich et al., 2008, 2011) and repeated determinations of active layer thicknesses (cf. GTN-P; https://gtnp.arcticportal.org/). Near-surface temperature for rocks with low ice contents is presently rising at fast rates of around 5°C per century (Noetzli et al., 2024). The slow process of heat diffusion at depth, however, causes strong and long-term paleoclimate effects (Noetzli and Gruber, 2009), especially where processes of latent heat exchange are involved. Deep permafrost warming has indeed now reached depths of many tens of meters (Etzelmüller et al., 2020).

The observed and ongoing deep warming, which affects temperature-dependent strengths of frozen rock masses, must have systematically reduced the stability of steep permafrost rock slopes. As a consequence, the frequency of rock-ice avalanches in icy mountains increases (Ravanel and Deline, 2011; Fischer et al., 2012; Coe et al., 2018). In the central Alps, average return times of large events with volumes of 10^6 m^3 or more reduced from 11 years between 1900 and 1980 to 5 years between 1980 and 2000 (Fischer et al., 2012; Metzger, 2026, see also https://www.permos.ch/data-portal/rock-falls). Since the turn of the century, eight more events were recorded: Dents du Midi in 2006, Dents Blanches in 2006 (Fischer et al., 2012), Cengalo in 2011 and in 2017, Fluchthorn in 2023, Scerscen in 2024 and Blatten in 2025. This further lowered the mean return time to about 3 years for these large events.

https://doi.org/10.5194/egusphere-2026-2821
Preprint. Discussion started: 6 July 2026

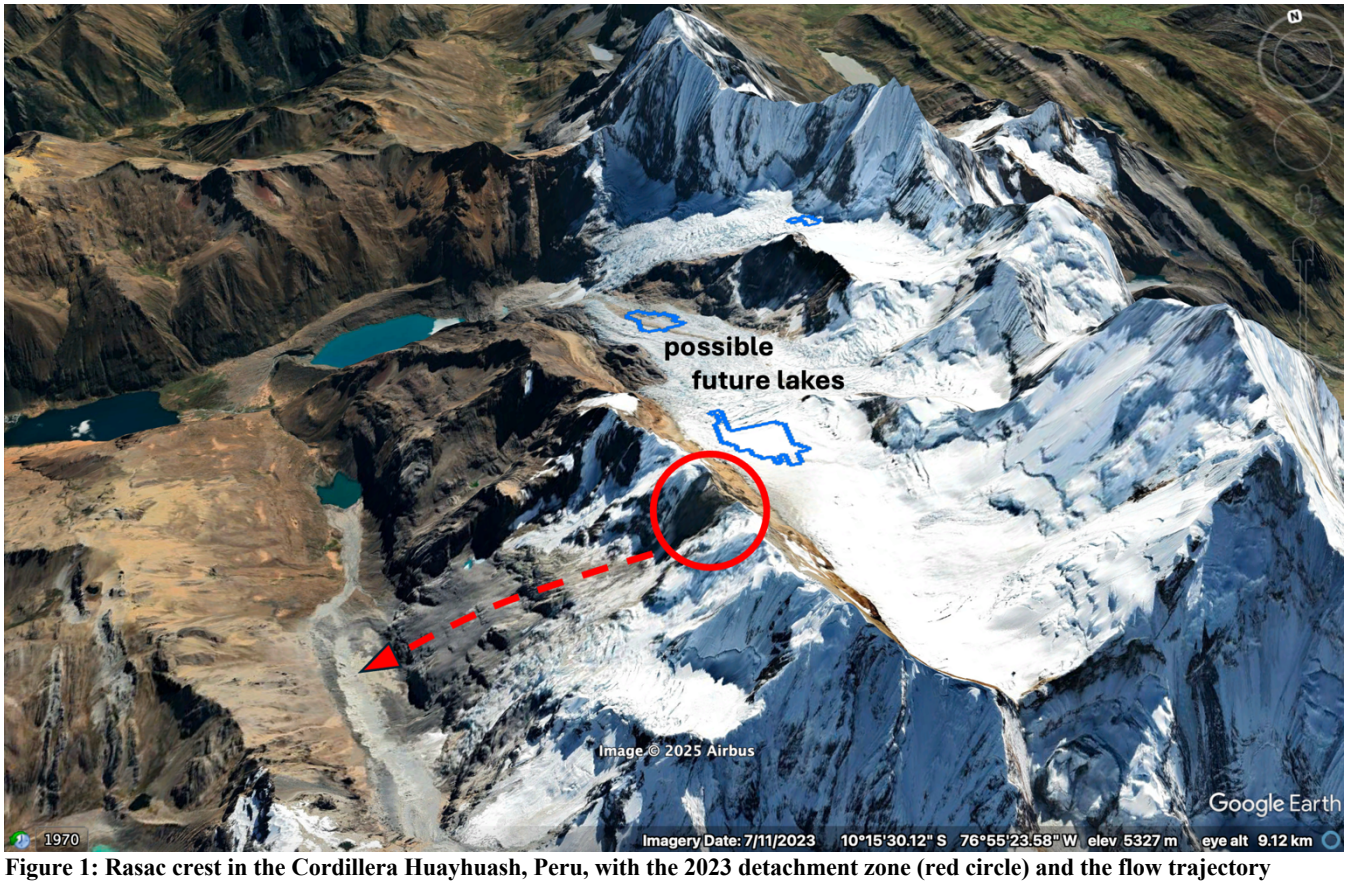

Figure 1: Rasac crest in the Cordillera Huayhuash, Peru, with the 2023 detachment zone (red circle) and the flow trajectory (dashed arrow) to the former Laguna Rasac. Possible future lakes (blue outlines at the glacier surface) are after Colonia et al. (2017) and Guardamino et al. (2019). The ice-clad peak at middle-right is Nevado Yerupajá, 6617 m, the second highest summit of Peru and the highest peak of the Amazon catchment. Background image © Google Earth.

Such landslides mostly occur in remote areas without impacting humans and causing damage to infrastructure (e.g., Rasac, Peru, Fig. 1). They can, however, also have catastrophic consequences far beyond historical precedence as most recently recorded at the multi-century old village of Blatten, Swiss Alps (Fig. 2). Where they transform into far-reaching process chains, they can cause heavy damage over large distances (Walter et al., 2020; Shugar et al., 2021), especially where they reach new lakes, create impact and flood waves, and lead to the formation of new landslide-dammed lakes (Carey et al., 2012; Haeberli et al., 2017; Sattar et al., 2023, 2025). Hazard zones can thereby extend to previously safe areas of human livelihood and infrastructure, thereby increasing risks beyond historical precedence (Fan et al., 2025).

The progressive and long-term worldwide destabilization of frozen high-mountain peaks is a serious consequence of global warming even though still not recognized by many. There are two reasons for the latter: (1) The processes developing at depth below mountain surfaces are not directly observable through visual inspection, and (2) they relate to slow heat diffusion at depth, which is further decelerated by latent heat exchange and decreasing energy availability at depth, in

https://doi.org/10.5194/egusphere-2026-2821
Preprint. Discussion started: 6 July 2026

combination causing extended delays but also long-term future commitments. A possibility to deal with such communication challenges is to appreciate the physical processes at play, to utilize numerical modelling of transient thermal conditions in complex mountain topography (Noetzli and Gruber, 2009), and to connect the results with empirical relations between changes in negative temperatures and stability.

The following illustrates the possibilities of using such a combined transient modeling of temperature changes and related thermally induced stability changes inside cold mountains over extended time periods (decades, centuries). We use the examples of the Rasac crest in the Cordillera Huayhuash of Peru (Fig. 1), where a large rock-ice avalanche took place from a permafrost slope in February 2023 (Emmer et al., 2025), and of Blatten, Valais Alps, Switzerland (Fig. 2), where a large rock-ice avalanche from a permafrost slope destabilized a glacier and destroyed a century-old village on 28 May 2025 (Büntgen et al., 2025; Fan et al., 2025).

A brief description is first given of the Rasac site with the 2023 landslide into a moraine-dammed lake, and of the catastrophic Blatten case in 2025. Present-day thermal conditions at the surface of the mountains are then assessed. This step needs the application of large-scale climate information and local modifications caused by topo- and microclimatic aspects. Using this information, past (Little Ice Age, LIA) colder surface temperatures are reconstructed in order to enable transient forward model calculations of present-day conditions at depth and related temperature and stability changes below surface. As a next step, corresponding developments for the remaining part of the 21st century can be simulated. Due to the complexity of the involved geotechnical and hydraulic aspects, the results can only be interpreted in a half-quantitative way but nevertheless enable important insights. The parameterization and modeling study presented here relates to pre-failure conditions at a remote site (Rasac 2023, Peru) with sparse available information, and at a site in densely populated mountains (Blatten 2025, Swiss Alps) with more detailed information. The main objective is to demonstrate procedures that provide a basic understanding of climate-influenced permafrost – particularly with respect to scales in space and time – and its relationship to slope stability issues in cold mountainous regions.

2 The sites: Rasac ridge with the 2023 rock-ice avalanche and Blatten with the 2025 rock-ice avalanche

Rasac ridge in the Cordillera Huayhuash of Peru (Fig. 1) is a NNW-SSE oriented, high-altitude, largely ice-clad bedrock ridge near Nevado Yerupajá, which with its elevation of 6617 m is the second highest summit in Peru and the highest peak within the Amazon catchment. Emmer et al. (2024) provide a detailed description and analysis of the rock-ice avalanche that took place in February 2023. Following several small-magnitude precursory events during the five years before failure, a

https://doi.org/10.5194/egusphere-2026-2821
Preprint. Discussion started: 6 July 2026

Figure 2: Rock-ice avalanche of 28 May 2025 which destroyed the multi-century old village of Blatten, Lötschental, Valais Alps, Switzerland. The sharp peak in the upper left is Bietschhorn 3934 m, the secondary crest and peak below it, from which the rock falls detached, is Kleines Nesthorn 3341 m. The brownish cloud in the detachment area indicates ongoing rockfall activity. The landslide-dammed lake at the lower left formed as a consequence of the deposits obstructing the main river of the valley. Photo ©swisstopo, 30.06.2025

https://doi.org/10.5194/egusphere-2026-2821
Preprint. Discussion started: 6 July 2026

total volume of about 1.1 to 1.5 million m3 detached at a mean altitude of about 5700 m from the steep slopes (> 45°) of the rock ridge with rock layers dipping near-parallel to the surface. The final detachment took place in cold permafrost with present-day mean annual surface temperatures estimated at about -5 to -6°C, while the precursory events started below the later detachment from only slightly warmer permafrost of perhaps about -4 to -5°C. The total landslide mass with an estimated ice content by volume of about 10 to 20% fell into Laguna Rasac at the foot of the mountain. The resulting flood wave and debris flow was contained within the Laguna Gochacotan located 3.5 km downstream (Emmer et al., 2025).

The catastrophic destruction of the historical village of Blatten on 28 May 2025 (Fig. 2) was caused by a process chain starting with the destabilization of a steep, multimillion m^3 permafrost rock mass at the secondary peak of Kleines Nesthorn, leading to a high frequency of minor and major rock falls onto the remnants of Birch glacier at the foot of the destabilized, rapidly moving and disintegrating frozen rocks. The extreme load exerted by the resulting talus cone of several million m^3 of deposited rock-fall debris finally destabilized the possibly polythermal but largely warm-based glacier, triggering a combined rock-ice avalanche of roughly 9 million m^3 with a rock to ice volume ratio of about 3:1 (Jacquemart et al., 2026). The centuries-old village of Blatten was almost completely destroyed. The damming of the valley in response to the ice-rock avalanche then led to the formation of a lake, impacting additional houses and infrastructure. Monitoring of the slopes had been initiated prior to the failure, allowing to evacuate Blatten's inhabitants prior to the catastrophic event.

3 Thermally induced stability changes of permafrost rock walls

Negative temperatures and frozen conditions have a strong influence on the geophysical, mechanical and hydraulic characteristics of rocks and rock masses (Davies et al., 2001; Krautblatter et al., 2012, 2013; Krautblatter and Leith, 2015). Freezing-induced increase in tensile and compressive strength of saturated rocks as well as in shear strength of ice-filled joints is substantial (Pfluger et al., 2025; Mamot et al., 2018). In addition, frozen joints and fractures limit the penetration of liquid water and reduce advective heat transfer and the development of hydrostatic pressures within the fractured rock mass. These processes add stability to steep rock slopes of cold mountains. Hence, average slope inclination under such conditions tends to be especially high (Kühni and Pfiffner, 2001).

Recent warming-induced degradation of permafrost rocks inverts such long-inherited stabilization effects. It reduces the shear resistance along rock joints by (i) reducing the fracture toughness of cohesive rock bridges, (ii) increasing pore pressures in the rock joints, thereby reducing effective stresses, (iii) lowering the friction along rock–rock contacts, (iv) enhancing the creep and likelihood of creep failure of ice infillings, and (v) reducing the fracture toughness of ice fillings and of rock–ice contacts (Krautblatter et al., 2013; Kuhn et al., 2025). The strength of ice in fractures especially decreases

https://doi.org/10.5194/egusphere-2026-2821
Preprint. Discussion started: 6 July 2026

where temperature approaches melting conditions of ice. Under such thermal conditions unfrozen water increasingly forms and interacts with ice and rock in complex ways (Davies et al., 2001; Gruber and Haeberli, 2007; Mamot et al., 2018, 2021; Kuhn et al., 2025). The full complexity of frozen rock-wall stability remains challenging to analyze in detail, especially for remote peaks without any in situ measured information. In the following, therefore, the simple and straightforward relation between Factors of Safety (FoS) and negative temperatures (°C) as derived from centrifuge experiments by Davies et al. (2001) (see Fig. 3) is used as a proxy in combination with 2D transient geothermal modeling and in a half-quantitative way. The main purpose is to illustrate long-term and deep-reaching subsurface effects on stability change from global warming. While the modeled time and depth scales can be considered to be quantitative, the degree of potential stability change must be seen to be largely relative/qualitative.

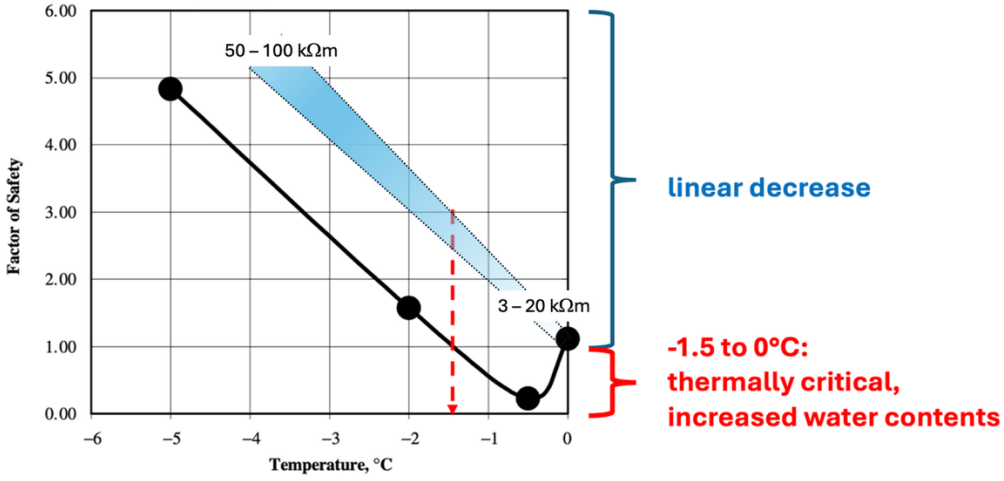

Figure 3: Stability of frozen rocks with ice-filled clefts as a function of rock temperature from centrifuge experiments; slope angle = 70°, inclination of discontinuity = 40°. The blue zone schematically indicates the characteristic temperature-dependent linear change in electrical resistivity after Krautblatter et al. (2010); Scandroglio et al. (2021); Mamot et al. (2021); a related change in P-wave velocities was documented by Krautblatter and Draebing (2014). Modified from Davies et al. (2001).

There are two important aspects in the empirical relation by Davies et al. (2001): its linearity and its strength. The linearity of the temperature/strength function for permafrost rocks is paralleled by strong, quasi-linear relations between negative temperatures and geophysical properties of frozen rocks: Seismic P-wave velocity (Krautblatter and Draebing, 2014) and electrical resistivity (Krautblatter et al., 2010; Scandroglio et al., 2021). The key physical effect involved most likely relates to the formation of a critical amount of "unfrozen water" in pores, microcracks and micro fissures already at negative temperatures (Krautblatter et al., 2013). Such documented linearity means that warming by a given amount causes the same change in warm as well as in cold permafrost rocks. This has important consequences for cases with mountain topography as the highest/coldest parts of ridges or peaks have the largest cumulative warming/weakening potential.

https://doi.org/10.5194/egusphere-2026-2821
Preprint. Discussion started: 6 July 2026

The observed linearity causes the gradient of negative temperatures versus strength to be approximately constant. The experiments of Davies et al. (2001) provide a gradient FoS °C^{-1} close to 1, reflecting a strong thermal effect on frozen rock mass stability in parallel to documented strong changes in geophysical properties as explained above. In their detailed application of thermally induced stability changes to a real mountain (Zugspitze, central Alps), Mamot et al. (2021) emphasize that the temperature of critical stability strongly depends on the inclination of the main fractures versus the slope angle. For slope angles > 30° they indicate values of 0.5 to 1 FoS °C^{-1}, which is comparable to the results of Davies et al. (2001). Mamot et al. (2021) also question as a possible artefact of the laboratory experiments by Davies et al. (2001) the existence of higher FoS for unfrozen than for ice-filled joints in the temperature range between -1.5 and 0°C. In the following, this temperature range is understood as a zone of increased effects from water circulating at depth.

The FoS is determined as the ratio between the resisting force and the driving force and can be defined as shown in Equation 1 for an infinite slope, which is used here for simplicity. The planar FoS is defined as

$$\mathrm{FoS} = \frac{\text{Resisting forces}}{\text{Driving forces}} = \frac{c'L + (W\ cos\,\theta - U)\ tan\,\varphi'}{W\ sin\,\theta} \quad (1)$$

where c' is the effective cohesion along the discontinuity, L is the length of the failure plane, W is the weight of the sliding block, θ is the dip of the discontinuity, U is the water pressure acting on the discontinuity, and φ' is the effective friction angle along the discontinuity.

Two cases may be evaluated: (i) shear through competent rock and (ii) shearing along a fracture or joint within the rock mass. The driving force within the competent rock remains unchanged and only the resisting force decreases in response to the temperature dependent decrease in rock strength. However, this decrease may not be substantial. Multiple processes are at play simultaneously as the temperature within an ice-filled fracture increases. First, the bond strength between the rock and the ice decreases as the thickness of the unfrozen water film increases. As warming continues, the water pockets within the fracture start to connect allowing the generation of pore pressures, which now act as new driving force and reduce the effective stresses, i.e. reducing the resisting forces. Elevated pore pressures can specifically form locally at temperatures close to zero degrees centigrade, as completely thawed conditions allow for them to dissipate and the resistance within a fracture is generated through the friction within that unfrozen joint. This explains why the FoS is generally the lowest at temperatures just below freezing when partially frozen conditions are present within the rock mass and not when the rock mass is completely thawed and elevated pore pressure allowed to dissipate.

The increase in pore pressures and in particular the rate at which the pore pressure increases within a rock mass is further accelerated through the penetration of heat with the water (advection). Depending on the initial temperature of the water and the characteristics of the rock mass the resulting penetration and impact of increased hydrostatic pressures can be substantial.

https://doi.org/10.5194/egusphere-2026-2821
Preprint. Discussion started: 6 July 2026

It is understood that local conditions vary and the above stated behavior may not always apply, but it highlights the complexity of evaluating the stability of cold mountain rock masses and the dynamic interaction between ice, water and rock.

To demonstrate the impact of the hydrostatic pressure in the rock mass stability at varying temperatures we evaluated the change in hydrostatic pressure that is required in order to reduce the FoS to 1.0 (Equation 1) at varying temperatures and angles of discontinuities (Fig. 4). We used the temperature dependent material properties for joints in limestone reported by Mamot et al. (2018). In thawed conditions, using an angle of friction of 35° and Equation 1, the FoS without water pressure would be 1.0, 1.2, 1.5 and 1.9 for joint angles of 35°, 30°, 25° and 20°, respectively. The water column that would reduce the FoS to 1.0 would be 0 m, 44 m, 62 m, and 75 m for the four joint angles, respectively. If the joint angle is steeper than 35°, the rock mass would only be stable under frozen conditions. For example, a joint angle of 35° would become stable at a temperature of -0.8°C, and an angle of 40° at -1.3°C, assuming there is no pore water pressure.

The combined effect of temperature and pore water pressure is summarized schematically in Fig. 5 where we are looking at the increase in hydrostatic pressure that is required to cause an instability for different joint angles at different temperatures, relative to the unfrozen conditions. For example, at a joint angle of 20°, the water pressure must be about

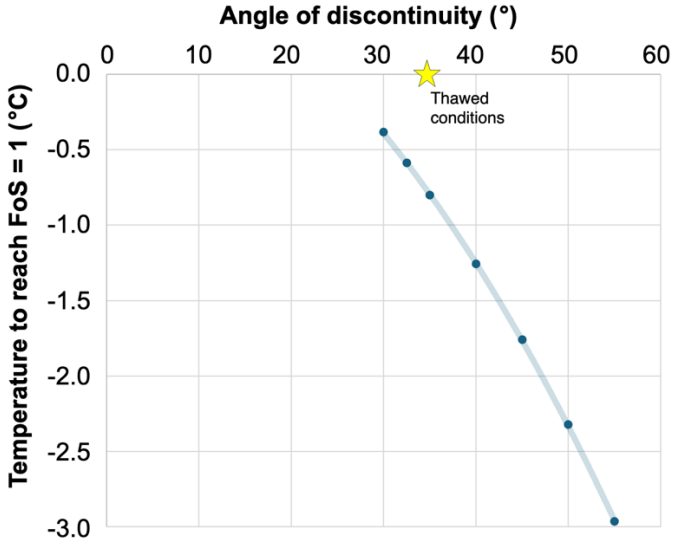

Figure 4: Temperature required to achieve stable conditions as a function of the discontinuity angle.

https://doi.org/10.5194/egusphere-2026-2821
Preprint. Discussion started: 6 July 2026

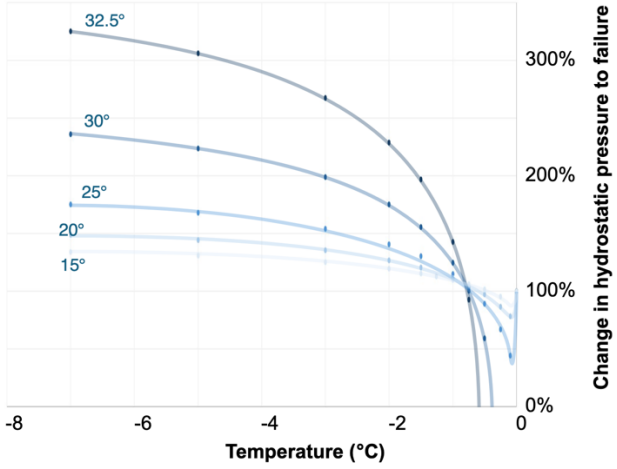

Figure 5: Change in the hydrostatic pressure with respect to unfrozen conditions that would be needed to trigger instability along a joint for different joint angles.

150% of the water pressure in the unfrozen conditions to trigger an instability at a temperature of -7°C. On the other hand, if the temperature is -0.5°C, a 97% water pressure is sufficient. Our analysis shows that the steeper the joint the more susceptible the stability becomes to changes in hydrostatic pressure. This is particularly critical close to the melting point of the ice in the discontinuities. At a temperature of -0.1°C only 45% of the unfrozen hydrostatic pressure would be required to trigger a failure of a 25° slope, while a 30° slope would not even be stable at all, as temperatures need to be -0.4°C or colder to generate stable conditions even without any pore water pressure.

The analysis underscores the sensitivity of frozen and partially frozen rock masses, noting that the resistance mobilized within a joint is influenced by geological conditions, temperature variations, and the ability of the rock mass to generate pore pressures along the failure plane.

4 Surface temperatures

In order to define complex subsurface temperature fields, surface temperatures must first be estimated. In rugged mountain topography with highly variable surface conditions, this can be quite challenging, requiring a differentiated procedure to be applied (Fig. 6). This procedure starts from large-scale and generally low-resolution climate information and related large-scale to regional-type model calculations of permafrost occurrence under present-day conditions such as, for instance, Boeckli et al. (2012a, b); Gruber (2012); Kenner et al. (2019); Obu et al. (2019); Baral and Haq (2020); Kim et al. (2024); Pandey et al. (2025). Local topo- and microclimatic aspects must then be considered in order to adjust this general information for effects of strong local variabilities in rugged topography. The derived surface temperatures provide a basis

https://doi.org/10.5194/egusphere-2026-2821
Preprint. Discussion started: 6 July 2026

for reconstructing past colder surface temperatures – here the Little Ice Age (LIA) before global warming – and for transient forward modeling of subsequent thermal evolution when strong paleo-effects persist at depth and influence long-term future conditions.

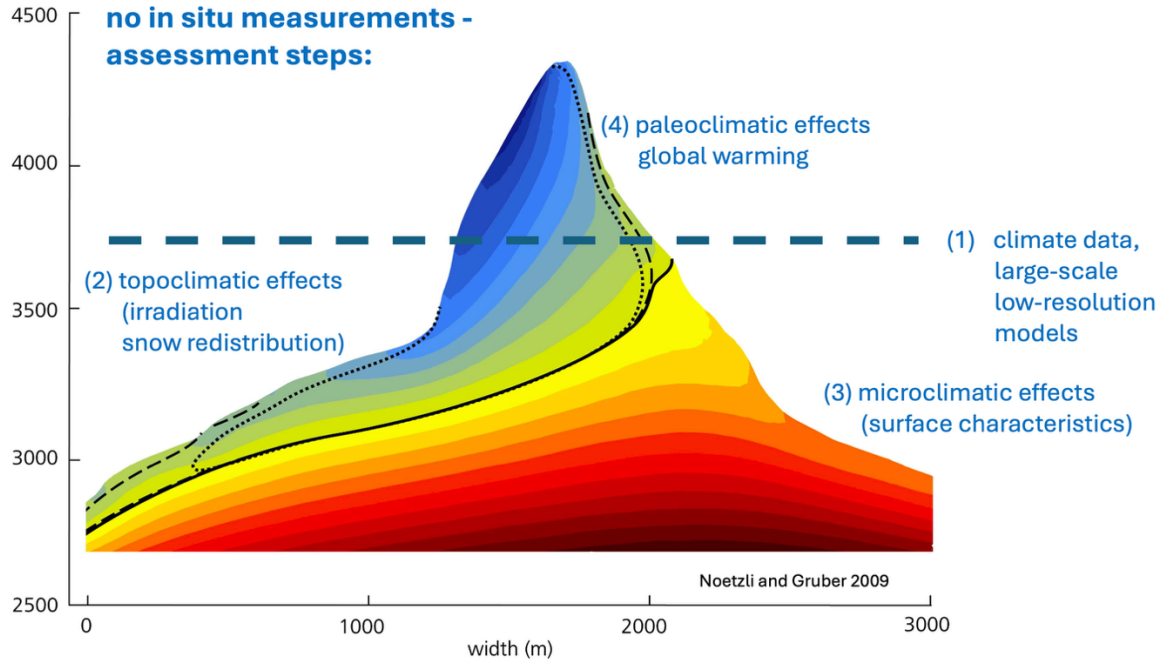

Figure 6: Principles of assessing present-day surface temperatures for remote peaks without in situ measurements. Modified from Nötzli and Gruber (2009).

Based on the permafrost distribution pattern modeled by BGC (Arenson et al., 2021), cold and deep permafrost is likely present near the summit of Yerupajá and Rasac (Fig. 7). Regional climate information about high altitude mean annual temperatures has been analyzed by Schauwecker et al. (2017). The freezing level height, or free air 0°C isotherm, as derived from multiple data types lies at 4900 m in the Cordillera Blanca to the North and at 5000 m in the Cordillera Vilcanota to the South. In the Cordillera Blanca, it has been rising by about 30 m per decade over the last 30 years. In the following, the 0°C annual isotherm is assumed to be 5000 m for the Rasac ridge in the year of the 2023 event. Applying an environmental lapse rate of 6 ± 2 °Ckm^{-1} (Stewart-Jones and Gruber, 2023) provides a rough estimate of the mean annual air temperature at the altitude of the detachment site at 5700 m of around 4 ± 2°C (Emmer et al., 2025). This important but low-resolution and strongly averaged result must be interpreted for local conditions by considering small-scale topo- and microclimatic aspects.

https://doi.org/10.5194/egusphere-2026-2821
Preprint. Discussion started: 6 July 2026

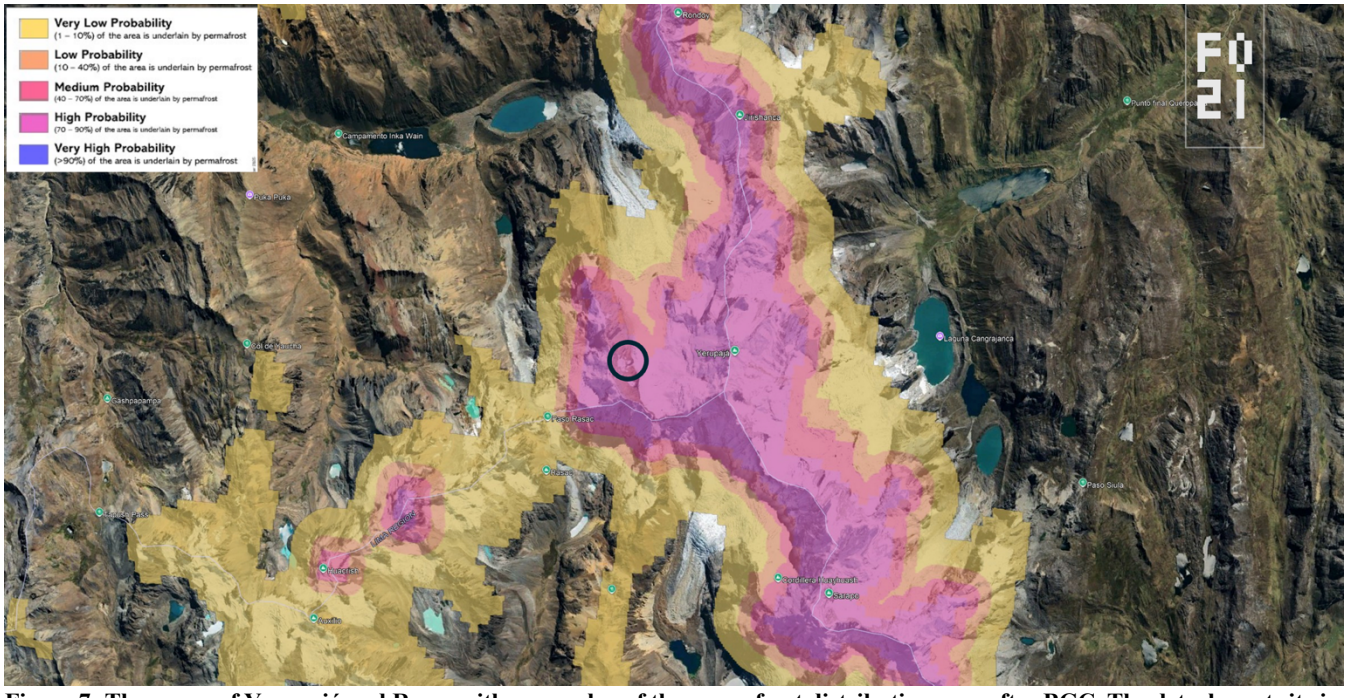

Figure 7: The group of Yerupajá and Rasac with an overlay of the permafrost distribution map after BGC. The detachment site is marked with a black circle. Background image Google Earth (Map data © 2026 Google Earth).

Local small-scale conditions as related to energy balance factors depend on topography (topo-climatic effects) and surface conditions (micro-climatic effects). Topography determines surface temperatures via altitude-dependent sensible heat and primarily aspect-dependent solar irradiation. The N-S difference in solar irradiation, which is predominant at mid-latitude, can be neglected at very low latitude and for a nearly N-S oriented ridge such as Rasac ridge. A pronounced E-W difference, however, is strikingly visible (Fig. 1): E-oriented slopes receive intense morning sun at generally low atmospheric humidity content, while W-oriented slopes are exposed to afternoon sun with often higher humidity content and clouds. At Rasac ridge like at many other summits – striking examples are, for instance, Pucaranra and Palcaraju above Laguna Palcacocha, Huaraz – high-altitude W-oriented slopes are often heavily ice-clad, while E-oriented slopes have no or at least much less ice cover. This, in turn, makes the surface albedo markedly lower on E-exposed slopes than on W-exposed slopes and, hence, reinforces this latitude-independent effect by enhancing the difference in absorbed direct solar irradiation. Based on early experience in the European Alps (Keller, 1992, cf. Emmer et al. (2025)), the related thermal difference can empirically be estimated at about 3°C. Lowering the temperature by half this value (1.5°C) on the colder W-exposed slope and correspondingly rising it by the same amount on the warmer E-exposed slope results in an estimated temperature at the 2023 detachment of -5.5 ± 2°C but of -2.5 ± 2°C at the same altitude on the warmer E-exposed side of the mountain. Such thermal asymmetries are quite common at sharp ridges and peaks (Noetzli et al., 2007).

https://doi.org/10.5194/egusphere-2026-2821
Preprint. Discussion started: 6 July 2026

Important additional effects are caused by microclimatic conditions (Fig. 8). Steep slopes with inclinations > 45° are especially cold, because no thick thermally insulating winter snow cover can form at their surfaces. Where covered by cold (and often millennia old), frozen-on ice aprons (Ravanel et al., 2023), such slopes are even further cooled down, because such ice surfaces cannot warm up above but cool down far below 0°C. Such ice aprons are, in fact, excellent and easily recognizable indicators for rock slope permafrost. Thermally more complicated are hanging glaciers with usually near-vertical, cold and frozen-on fronts but less inclined firn zones above the fronts. Such hydraulically permeable firn zones, where meltwater can infiltrate, refreeze and thereby warm up firn bodies at depth are known to be considerably warmer than massive ice bodies at the same altitude and in many cases are even temperate (Haeberli and Alean, 1985; Suter et al., 2001; Margreth et al., 2017). The resulting polythermal structure is likely to induce complex thermo-hydraulic conditions (Haeberli et al., 2004). The detachment zone of the 2023 Rasac event had been covered by strongly cooling ice aprons rather than thermally more complex hanging glaciers. It can therefore be concluded that the 2023 failure must have taken place within cold-deep permafrost.

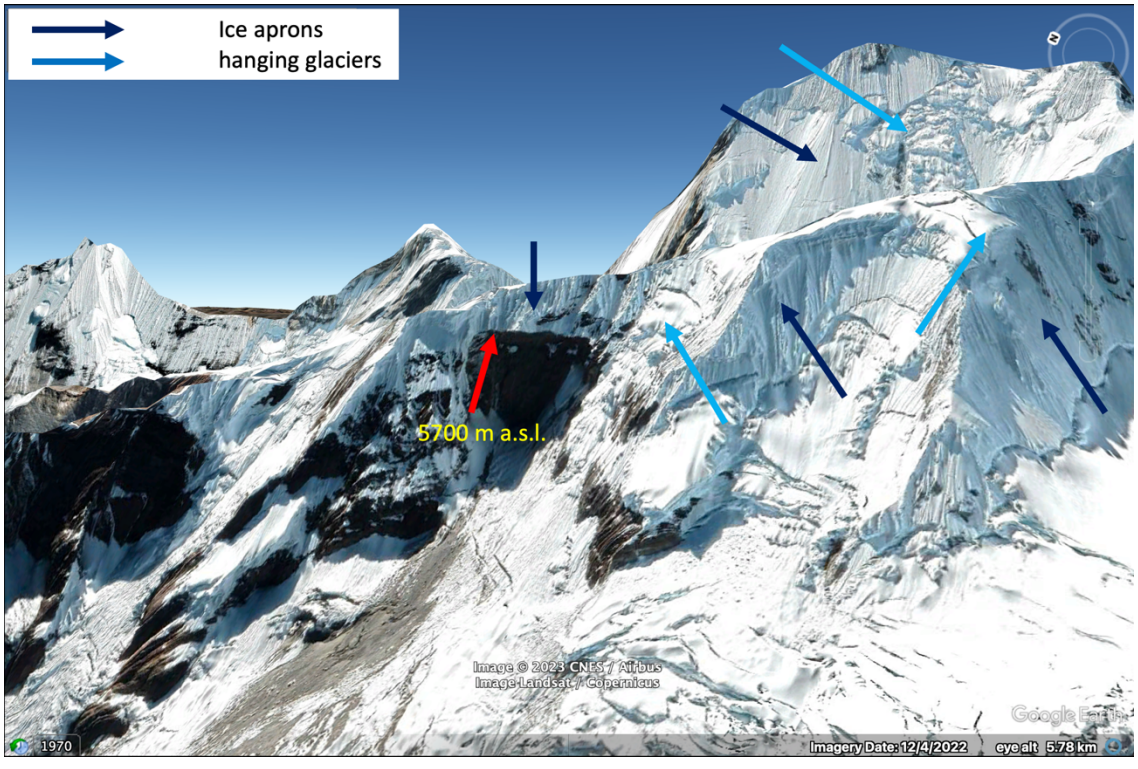

Figure 8: Surface ice at and around the detachment site of Rasac in the year before the main slide of 2023. Dark blue arrows point to cold, frozen-on ice aprons, while light blue arrows indicate hanging glaciers with more complex thermal structures. Note precursory event below later detachment of uppermost slope section with frozen-on ice aprons. Background image © Google Earth.

Permafrost conditions in the destabilized high-altitude rock wall at Kleines Nesthorn above Blatten can be inferred from numerical climate-related model calculations of permafrost occurrence such as Boeckli et al. (2012a) or Kenner et al. (2019).

https://doi.org/10.5194/egusphere-2026-2821
Preprint. Discussion started: 6 July 2026

330 The detailed and high-resolution model by Kenner et al. (2019) had been calibrated using borehole temperatures around the year 2010. It includes estimates of near surface mean annual temperatures in bedrock permafrost with low ice content and indicates sites of ice-rich permafrost (frozen talus/debris, moraines, rock glaciers).

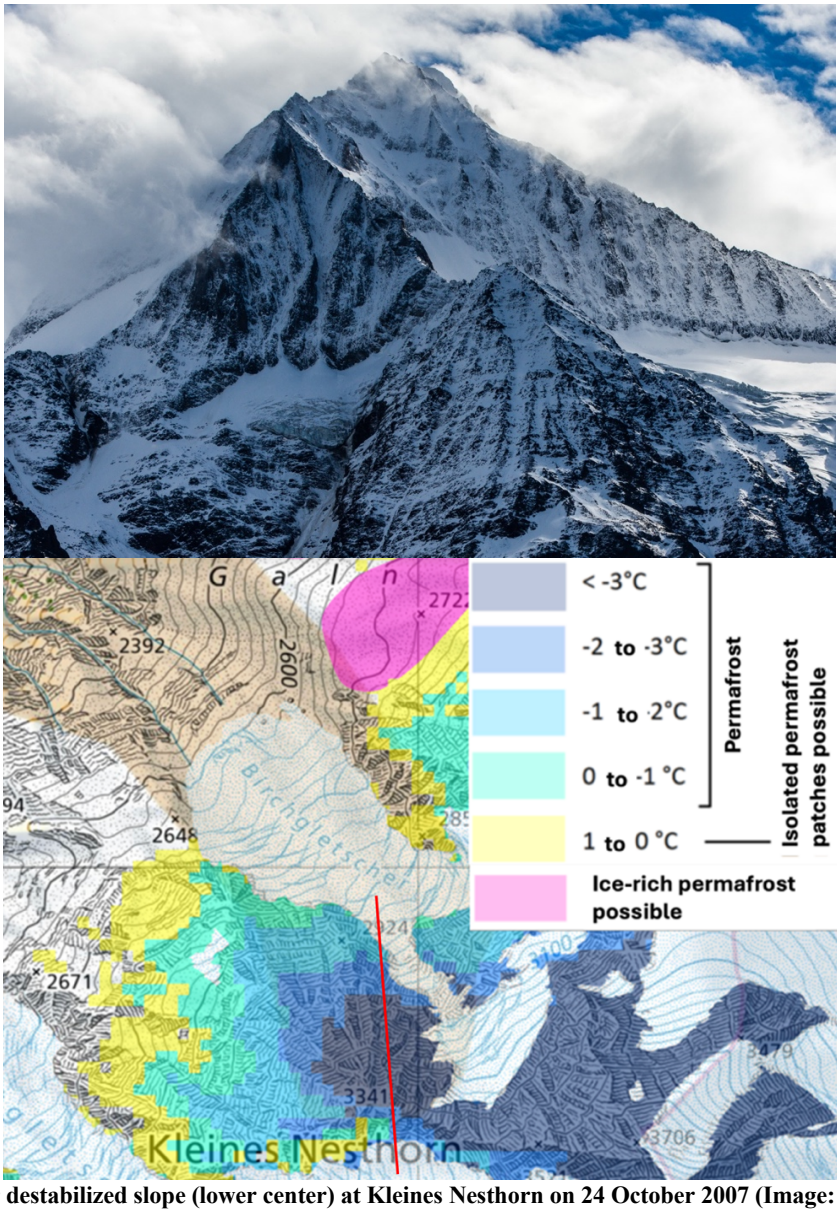

335 **Figure 9: Top: The later destabilized slope (lower center) at Kleines Nesthorn on 24 October 2007 (Image: Marco Volken). Bottom: Permafrost occurrence and characteristics at the later destabilized slope between Kleines Nesthorn and Birch glacier after Kenner et al. (2019). The thermally modeled profile is indicated by a red line. Source: SLF permafrost map; https://www.slf.ch/de/services-und-produkte/permafrost-und-bodeneiskarte**

340

https://doi.org/10.5194/egusphere-2026-2821
Preprint. Discussion started: 6 July 2026

For the north-oriented, now destabilized slope between Kleines Nesthorn and Birch glacier, the model of Kenner et al. (2019) (map publicly available at https://www.slf.ch/de/services-und-produkte/permafrost-und-bodeneiskarte/) is applied. This model distinguishes between ice-poor and ice-rich permafrost and was tested for the entire Swiss Alps. A linear regression formula based on elevation and potential incoming solar radiation for ice-poor ground (bedrock) predicts ground temperatures calibrated with data from borehole measurements around 2010 at multiple depths with an accuracy higher than 0.6 °C. Figure 9 indicates mean near-surface permafrost temperatures at the Kleines Nesthorn slope of less than -3°C on top to about -1°C at its bottom. Since LIA, the slope has remained free of surface ice (ice aprons, hanging glaciers; cf. old maps at https://www.swisstopo.admin.ch/en/a-journey-through-time-maps). Birch glacier at the foot of the slope used to be a steep mountain glacier exerting no major mechanical (buttressing) or thermal influence on the now destabilized slope. During recent years, Birch glacier increasingly disrupted by losing the connection with its former accumulation area (hanging glacier); before its recent burial and sudden end, it had transformed into what is called a “regenerated glacier” fed through ice avalanches from the disconnected upper hanging glacier and becoming increasingly debris-covered as a consequence of rock falls from the later destabilized Nesthorn slope. Warm to potentially even no permafrost is indicated in places at the sun-exposed south-oriented steep slope directly behind the crest. Such strongly asymmetric thermal conditions with near horizontal heat flow components and the potential access to surface water are characteristic for many ridge sites and peaks of rugged mountains. Such conditions also offer pathways for complex hydro-geological conditions.

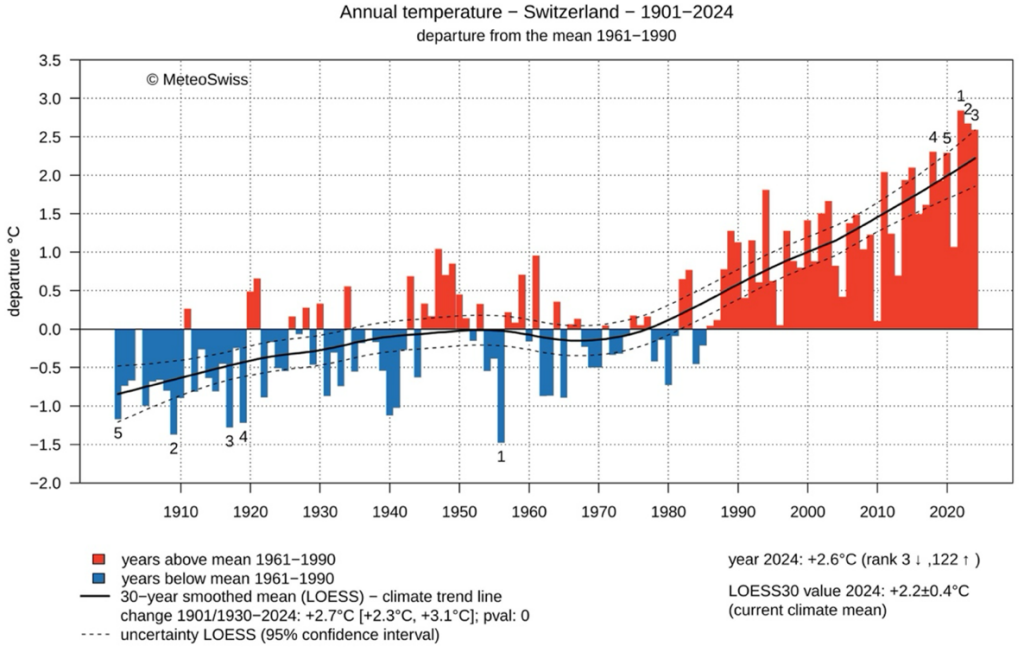

Figure 10: Mean annual air temperature in Switzerland 1901-2024: Departure from the mean. Source MeteoSwiss.

https://doi.org/10.5194/egusphere-2026-2821
Preprint. Discussion started: 6 July 2026

With this information about present temperature conditions, surface temperatures can now be set back to past colder conditions in order to apply transient forward model calculations of present-day conditions as affected by rising global temperatures but with strongly delayed paleo-effects at depth.

Thermal equilibrium conditions during preindustrial time and the LIA are assumed as a realistic-pragmatic assumption for assessing impacts from global warming on thermal conditions inside perennially frozen mountains. As no long-term observations on mean annual air temperatures (MAAT) is available for high altitudes in the Peruvian Cordilleras, well documented quantitative information from the Swiss Alps is used as a proxy. Around 2010, mean annual air temperature in Switzerland was about 2°C higher than in the preindustrial time of 1870-1900 and further increased since then by almost 1°C (https://www.meteoswiss.admin.ch/climate/climate-change.html; (cf. Fig. 10). We use this value as a best estimate for the temperature difference LIA/2010 and 2023/2025, also for the Rasac site. Rates of change in near-surface temperatures of bedrock permafrost are similar to those in mean annual air temperature and in non-frozen boreholes (Noetzli et al., 2024). The latest decade is characterized by extraordinary warming (MAAT about +0.9°C, +0.5°C for bedrock permafrost and non-frozen ground).

5 Thermal permafrost modeling with rugged topography

We model the two-dimensional thermal evolution of Alpine permafrost using the open-source multi-physics software Elmer (Råback et al., 2020). The simulations consider heat transfer by conduction only, neglecting latent heat effects associated with phase changes, as the volumetric fraction of ice or water in pores and fractures is here assumed to be negligible. The rock mass is treated as a homogeneous and isotropic medium with constant physical properties.

Initial surface temperature conditions incorporate spatial variability related to elevation and to slope aspect (i.e., the orientation of the rock faces relative to incoming solar radiation and to climatic conditions, see Section 4). Specifically, a temperature offset of 3 C is prescribed between opposing aspects: north–south faces for Kleines Nesthorn and west–east faces for Rasac. This parameterization approximates the influence of differential solar irradiance on surface temperatures. Combined with a reference temperature and an atmospheric lapse rate, this approach defines the initial temperature distribution along the upper boundary.

https://doi.org/10.5194/egusphere-2026-2821
Preprint. Discussion started: 6 July 2026

	Rasac	Kleines Nesthorn
Physical property		
Density ($kg\,m^{-3}$)	2400	2400
Thermal conductivity ($W\,m^{-1}\,°C^{-1}$)	2	2
Specific heat capacity ($J\,kg^{-1}\,°C^{-1}$)	800	800
Initial conditions		
Temperature (west/north) (°C)	−7	−5
Temperature (east/south) (°C)	−4	−2
Reference elevation (m)	5700	3319
Atmospheric lapse rate ($°C\,km^{-1}$)	6	6
Boundary conditions		
Geothermal heat flow ($mW\,m^{-2}$)	30	65
Lapse rate ($°C\,km^{-1}$)	6	6
Temperature change 1850–2010 (°C/100 y)	1.25	1
Temperature change past 2010 (°C/100 y)	6.6	5

Table 1: Rock physical properties for both Rasac and Kleines Nesthorn

To solve the two-dimensional temperature field, boundary conditions include a prescribed geothermal heat flux at the base of the domain and a time-dependent surface temperature forcing. A steady-state solution corresponding to Little Ice Age (LIA, circa 1850) conditions is first computed. This field is then used as the initial condition for a transient simulation spanning 150 years (1850–2010). For Kleines Nesthorn, the simulation is extended by an additional 15 years (2010–2025) using a larger surface warming rate. For Rasac, the simulation is extended until 2100. Table 1 summarizes the physical properties, initial conditions, and boundary conditions used for both Rasac and Kleines Nesthorn.

6 Results

The modeled LIA steady-state temperature field for both, Rasac (Fig. 11a) and Kleines Nesthorn (Fig.12a), show cold and deep permafrost with a pronounced asymmetry: east-west in the case of Rasac and north-south in the case of Kleines Nesthorn. Near surface temperatures are several degrees below zero and permafrost reaches down to maximum depths of several hundred meters. The two ridges are essentially frozen throughout, including their warm sides.

Forward calculation of present temperature fields from such reconstructed LIA conditions document that global warming

https://doi.org/10.5194/egusphere-2026-2821
Preprint. Discussion started: 6 July 2026

since preindustrial time induced warming at depth down to roughly about 100 m below surface (Figs. 11b, 12b, c). In accordance with earlier model calculations (Noetzli and Gruber, 2009) and long-term observations of borehole temperatures (Etzelmüller et al., 2020; Koenig et al., 2025), strongest increase of subsurface temperatures has taken place in the uppermost about 50 m below surface (Figs. 11d, e, 12d - f). Vertical temperature gradients and related heat flow strongly reduced correspondingly.

Figure 13 shows the vertical temperature profile underneath the summit of the Kleines Nesthorn and its first and second gradients with depth. The thermal profile representative of LIA conditions (around 1850) exhibits a near-constant positive temperature gradient, consistent with a quasi-equilibrium state between atmospheric forcing and the ground thermal regime; while such equilibrium conditions likely never existed in a strict sense, they provide a reasonable baseline for the initial condition of the forward numerical model. Toward more recent years, the progressive reduction of the gradient and its eventual inversion highlight the pronounced lag of the thermal regime at greater depths in responding to rapidly evolving atmospheric conditions. The unprecedented atmospheric temperature rise of the 20th and early 21st century further influences this lag, which is high-lighted in the temporal derivative of the thermal gradient. It demonstrates a marked acceleration in the rate of gradient change under ongoing global warming. Importantly, this subsurface response is expected to differ substantially from the approximated linear air-temperature trends observed over recent decades (e.g., 2010 - 2025), reflecting the depth-dependent thermal inertia of the rock mass. Collectively, these observations indicate that permafrost temperatures in bedrock are increasingly unable to keep pace with atmospheric warming, marking the onset of significant thermally driven, and consequentially hydrologically induced, changes in high mountain environments. The presence of latent heat effects, controlled by the amount of ground ice present mainly in rock fractures, further increases the complexity of this response by moderating and delaying thermal adjustment rates.

The permafrost base of such cold/deep permafrost, however, still largely remains at its LIA steady-state condition. This strong, long-term paleoclimatic effect and retardation becomes obvious when the transient temperature field is compared with a steady-state calculation for modern conditions: Ignoring paleo-effects leads to strong underestimations of permafrost extents below surface (Figs. 11d and 12d).

In the Rasac case, the only marked change in the permafrost extent is the upward shift of the permafrost lower altitudinal limit in the lower reaches of the west-oriented slope and in the east-oriented summit slope, inducing near-surface (active layer) thawing while permafrost in disequilibrium with climatic conditions continues to exist at depth for some time. In the Nesthorn case, a remarkable change concerns the south-exposed slope, where permafrost may have started to disappear, thereby facilitating water penetration deep into the mountain. In both cases, however, the LIA permafrost base at depth largely remained in place. The detachment of the landslides took place within the frozen and still quite cold zone of the slopes.

https://doi.org/10.5194/egusphere-2026-2821
Preprint. Discussion started: 6 July 2026

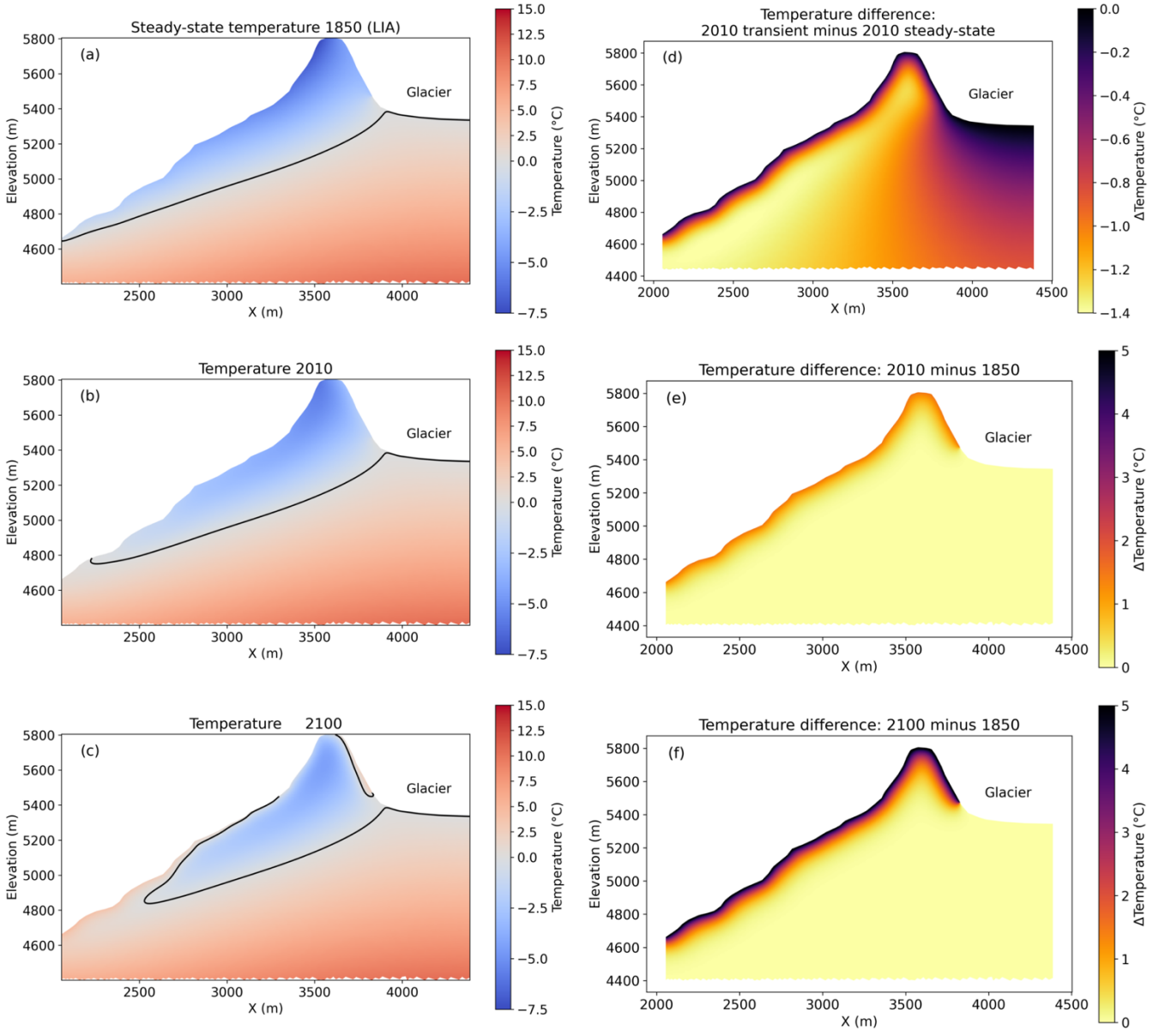

Figure 11: Modeled thermal field at Rasac: (a) Steady-state LIA, (b) transient 2010, (c) transient 2100, (d) paleoclimate effect (transient 2010 minus stead-state today), (e) temperature difference between 2010 and LIA, and (f) temperature difference between 2100 and LIA. Black contour in (a) – (c) is 0°C isotherm. West is to the left.

https://doi.org/10.5194/egusphere-2026-2821
Preprint. Discussion started: 6 July 2026

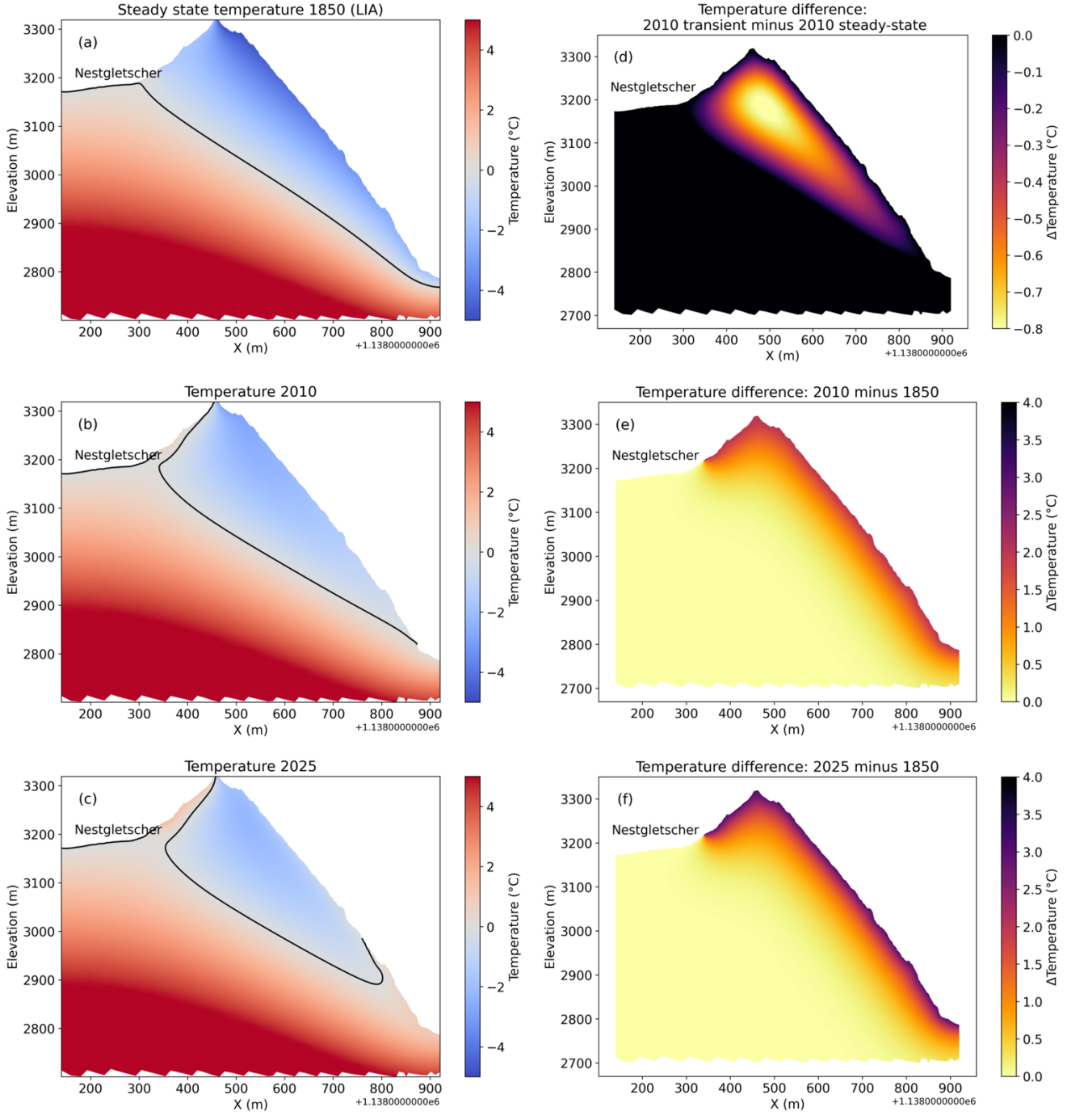

Figure 12: Modeled thermal field at Kleines Nesthorn: (a) Steady-state LIA, (b) transient 2010, (c) transient 2025, (d) paleoclimate effect (transient 2010 minus stead-state 2010, (e) temperature difference between 2010 and LIA, and (f) temperature difference between 2025 and LIA. Black contour in (a) – (c) is 0°C isotherm. North is to the right.

https://doi.org/10.5194/egusphere-2026-2821
Preprint. Discussion started: 6 July 2026

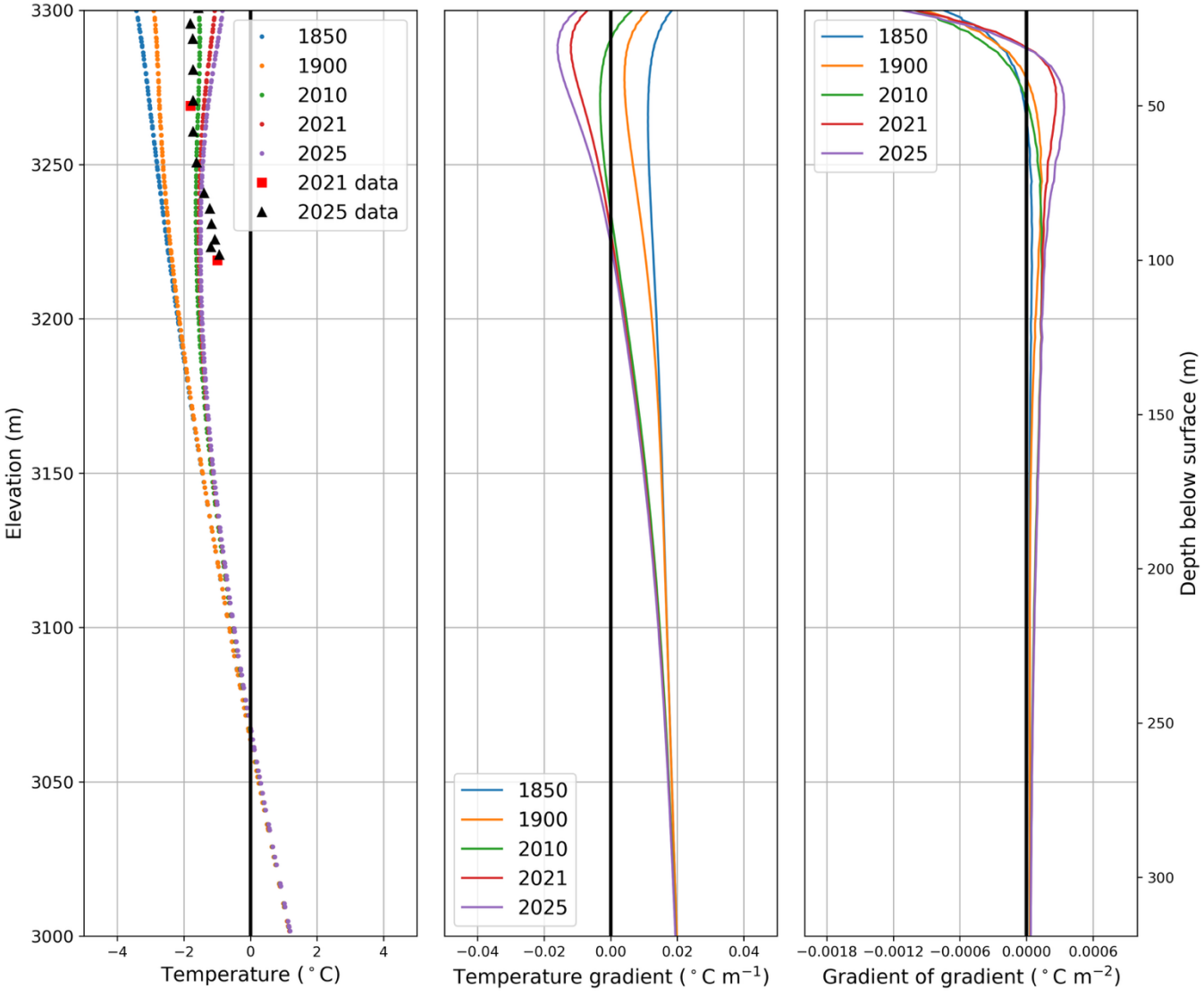

Figure 13: Profile of temperature and first and second gradients of temperature for Kleines Nesthorn below 3300 m. The 2021 and 2025 data refer to borehole temperatures measured at Stockhorn above Zermatt (data from PERMOS data portal: https://www.permos.ch/data-portal/permafrost-temperature-and-active-layer)

7 Further heating and thermally induced stability change

For the Rasac case, continued warming until the end of the century was calculated using an assumed additional temperature increase of +5 C (Fig. 11c, f). Future warming effects were not calculated for the Kleines Nesthorn because of the massive change in surface geometry of the slope induced by the destabilization and avalanching. The effect of the extremely warm years since 2010 was modeled and shown to primarily affect the uppermost about 30 meters below surface (see Fig. 13).

https://doi.org/10.5194/egusphere-2026-2821
Preprint. Discussion started: 6 July 2026

These extremely warmed up and mechanically weakened frozen rock parts were eliminated by the May 2025 event.

8 Discussion

The results presented here provide a general overview of the spatiotemporal scales related to permafrost thermal conditions with their warming-induced potential stability reduction of the involved high-altitude frozen rocks. Uncertainties thereby primarily concern ice contents with their effects on thermal characteristics (diffusivity/conductivity) of the frozen rocks, latent heat effects due to melting ice components, and influence of pore water as it controls advective heat transfers and effective stresses. From borehole temperature data in the Swiss Alps, Weber et al. (2025) empirically derive median diffusivity values of 1.5 ± 0.6 mm^2 s^{-1} for frozen rocks with low ice content and 1.3 ± 0.3 mm^2 s^{-1} for ice-bearing bodies like ice-supersaturated viscous creep features (rock glaciers) in frozen debris. This provides an assessment of the related uncertainty ranges. Corresponding sensitivity analyses could be carried out but would have limited effects on the general characteristics of the here presented results.

Stronger and more uncertain effects must be expected from latent heat exchange through melting of ice in frozen rocks. For deep/perennial freezing of bedrock after the vanishing of a warm-based glacier (Aletsch), Wegmann et al. (1998) showed that even small ice contents of 3% and 6% by volume exert strong retarding effects at depth, as it takes five to ten times more energy to melt even such small amounts of ice compared to simply changing its temperature by one degree. This is necessitating calculations over millennial time scales for approaching new equilibrium conditions. As quantitative information about subsurface ice contents is not generally available, considerable uncertainties remain. Sensitivity analyses should assume higher ice contents in the uppermost about 30 m below surface, where cracks and fissures, often formed by thermally induced stresses within the rock mass, are largest and most abundant (cf. Krautblatter et al., 2013). Corresponding effects can be expected to be greatest, where permafrost temperatures are close to 0°C, allowing for ice and unfrozen water to co-exist. Due to such latent heat effects, permafrost thaw at the sun-exposed slope of Kleines Nesthorn above Blatten (cf., Fig. 12b, c) may not yet have been completed, preventing or partially reducing penetration of water at depth. Ice-bearing rocks have indeed been visually observed there (C. Lambiel and L. Ravanel, personal communication). In the same way, permafrost thawing at the foot of the north slope may have been less than modeled without ice content. Thawing of permafrost rocks in warm parts of the slopes in question are, however, likely to continue and to further enable water infiltration deep inside the mountain generating pore water pressures and reductions in the rock mass stability. This aspect opens an important but complex and difficult field of thermal, hydrological, and stability analyses, including efficient advective heat transport at depth with its dramatically different time and depth scales (Haeberli et al., 1997; Gruber and Haeberli, 2007; Offer et al., 2025). In the commonly existing absence of precise information about high-resolution evolution

https://doi.org/10.5194/egusphere-2026-2821
Preprint. Discussion started: 6 July 2026

in time of temperatures deep inside past or potential future detachment zones in permafrost rocks, realistic assumptions and plausibility considerations can be reasonably applied rather than exact treatments.

Such limitations make thermo-hydro-mechanical (THM) analyses of detachment zones of landslides from steep bedrock permafrost half-quantitative. Corresponding model results nevertheless provide essential insights and help overcoming the still often lacking awareness about the "hidden phenomenon" of mountain permafrost in the communication with the public, policy makers, political authorities or scientists from other disciplines. The idea, for instance, that climate-induced "permafrost thaw" reduces the stability of frozen rock slopes is not wrong but to some degree a misleading simplification. It is "permafrost degradation", the integrative effect of deep warming, infiltration of water, and thawing, which is the essential climate impact. In contrast to complete thawing, which in many cases involves time scales of centuries and millennia, deep climate-induced warming with related stability changes already takes place within decades and likely continues for centuries and millennia to come. Simple stability assessment already highlight that the hydrostatic pressures needed to generate unstable conditions may, depending on the rock mass characteristics, be relatively low. Permafrost depths under present-day conditions still largely reflect past colder conditions, while temperatures in the upper about 100 meters are determined by effects of intensive global warming.

Destabilization of steep, perennially frozen rock slopes is a multi-factor phenomenon, where geology, topography, and climate history together play key roles. For individual cases, therefore, climate-induced permafrost degradation and related mechanical weakening must be considered to be an important contributing factor but never constitutes the one and only influence. The situation is different for the development in time of landslide occurrence in cold mountains. In contrast to geological and topographic effects, the time scale of effects from degrading permafrost reflects the time scale of global warming. A frequency increase at decadal time scales of large landslides from icy peaks can only be explained by climate impacts on thermal characteristics and related stability conditions of frozen rock slopes. Statistically quantifying the impact of climate change on frequency (recurrence times / annual probabilities) and magnitudes of large mass movements remains challenging because of limitations in the available datasets (Jacquemart et al., 2024). The numerous documented recent events, however, constitute a serious warning. As atmospheric temperature rise as well as its effects on temperatures at depth below surface and on the stability of frozen mountain slopes continue, this development could well be irreversible for many future generations.

9 Conclusions

This study demonstrates that transient, climate-driven thermal evolution of high-mountain permafrost rock walls fundamentally alters slope stability on different spatial and temporal scales that are directly relevant for present and future

https://doi.org/10.5194/egusphere-2026-2821
Preprint. Discussion started: 6 July 2026

hazard and risk assessments. Using a semiquantitative modelling framework applied to the Rasac (Peru, 2023) and Blatten (Swiss Alps, 2025) events, we show that recent large rock-ice avalanches occurred not as a result of complete permafrost thaw, but within still cold and deep permafrost that has undergone substantial degradation due to long-term warming and delayed subsurface thermal adjustment.

The results highlight the critical role of paleoclimatic memory. Present-day temperature fields in steep permafrost rock walls continue to reflect Little Ice Age thermal conditions at depth, while the upper tens of meters respond rapidly to recent decades of unprecedented atmospheric warming. This topographically driven thermal disequilibrium produces zones of enhanced mechanical sensitivity, particularly where temperatures approach the melting point of the pore ice and small changes induce disproportionately large reductions in effective rock-mass strength. Ignoring paleo-effects and assuming modern steady-state conditions leads to a systematic underestimation of permafrost extent and misrepresentation of stability conditions at depth.

We demonstrate that low overall ice content does not imply low hazard potential. Even limited amounts of ice within fractures exert a first-order control on both mechanical behavior response and impact on rock mass hydrology. As warming progresses, partial thawing promotes the formation of unfrozen water films, enhances permeability, and enables infiltration of surface and meltwater. Simple stability considerations already indicate that the hydrostatic pressures required to generate unstable conditions can, depending on fracture geometry and rock-mass properties, be relatively low. Consequently, thermo-hydro-mechanical (THM) interactions within the rock mass, rather than temperature changes alone, must be regarded as central to understanding destabilization processes in degrading permafrost rock walls.

The comparison between Rasac and Blatten further underlines that similar physical mechanisms operate across very different climatic, geological, geographical, and environmental settings. While absolute material properties and boundary conditions differ, the governing controls, such as warming at depth, delayed thermal response, ice in fractures and fissures, and hydro-mechanically driven weakening due to pore pressure build-up, remain consistent. This supports the broader applicability of the presented modelling approach as a process-oriented tool for interpreting past events and identifying potentially unstable zones in other high-mountain regions.

From a hazard perspective, the observed recent increase in the frequency of large rock-ice avalanches cannot be explained by geological or topographic factors alone. Changes in recurrence times and annual probabilities on decadal time scales are most plausibly linked to climate-induced permafrost degradation. While statistical quantification remains challenging due to limited inventories, the growing number of well-documented events constitutes a clear warning signal. As atmospheric warming continues, further increases in both rockfall frequency and potentially magnitude must be expected. This is

https://doi.org/10.5194/egusphere-2026-2821
Preprint. Discussion started: 6 July 2026

particularly concerning for locations where unstable slopes interact with glaciers or lakes and generate cascading process chains.

Finally, this study underscores the need to better communicate the nature of permafrost-related hazards to practitioners, policy makers, and affected communities. The destabilization of frozen rock walls is a largely hidden, long-term process with potentially severe consequences. Incorporating transient permafrost dynamics and coupled thermal–hydrological effects into hazard assessments is therefore essential for realistic risk assessment and for developing effective adaptation and mitigation strategies in high-mountain regions under ongoing climate change.

Author contributions: WH developed the concept of the study, DC carried out the numerical model calculations and LA treated the geotechnical aspects. All three together discussed the results and wrote the text.

Competing interests: No competing interests are present.

Code and data availability: There is no code to declare.

Acknowledgements: Acknowledgements will be added after the review process.

Financial support: No outside support was received.

References

Arenson, L. U., Pino, C., Schimnowsky, M., Wainstein, P. A., and Cecioni R., A.: A Continental Permafrost Distribution Model for the South American Andes, in: Regional Conference on Permafrost and 19th International Conference on Cold Regions Engineering, 2021.

Baral, P. and Haq, M. A.: Spatial prediction of permafrost occurrence in Sikkim Himalayas using logistic regression, random forests, support vector machines and neural networks, Geomorphology, 371, 107 331, https://doi.org/10.1016/j.geomorph.2020.107331, 2020.

Boeckli, L., Brenning, A., Gruber, S., and Noetzli, J.: A statistical approach to modelling permafrost distribution in the European Alps or similar mountain ranges, The Cryosphere, 6, 125–140, https://doi.org/10.5194/tc-6-125-2012, 2012a.

Boeckli, L., Brenning, A., Gruber, S., and Noetzli, J.: Permafrost distribution in the European Alps: calculation and evaluation of an index map and summary statistics, The Cryosphere, 6, 807–820, https://doi.org/10.5194/tc-6-807-2012, 2012b.

https://doi.org/10.5194/egusphere-2026-2821
Preprint. Discussion started: 6 July 2026

Büntgen, U., Oppenheimer, C., Farinotti, D., Nahtz, T., and Esper, J.: The 2025 Blatten disaster in the Swiss Alps followed exceptional warming and highlights the vulnerability of people and heritage in glaciated landscapes, Communications Earth & Environment, 6, 994, https://doi.org/10.1038/s43247-025-02994-8, 2025.

Carey, M., Huggel, C., Bury, J., Portocarrero, C., and Haeberli, W.: An integrated socio-environmental framework for glacier hazard management and climate change adaptation: lessons from Lake 513, Cordillera Blanca, Peru, Climatic Change, 112, 733–767, https://doi.org/10.1007/s10584-011-0249-8, 2012.

Coe, J. A., Bessette-Kirton, E. K., and Geertsema, M.: Increasing rock-avalanche size and mobility in Glacier Bay National Park and Preserve, Alaska detected from 1984 to 2016 Landsat imagery, Landslides, 15, 393–407, https://doi.org/10.1007/s10346-017-0879-7, 2018.

Colonia, D., Torres, J., Haeberli, W., Schauwecker, S., Braendle, E., Giraldez, C., and Cochachin, A.: Compiling an Inventory of Glacier-Bed Overdeepenings and Potential New Lakes in De-Glaciating Areas of the Peruvian Andes: Approach, First Results, and Perspectives for Adaptation to Climate Change, Water, 9, https://doi.org/10.3390/w9050336, 2017.

Davies, M. C. R., Hamza, O., and Harris, C.: The effect of rise in mean annual temperature on the stability of rock slopes containing ice-filled discontinuities, Permafrost and Periglacial Processes, 12, 137–144, https://doi.org/10.1002/ppp.378, 2001.

Emmer, A., Vilca, O., Salazar Checa, C., Li, S., Cook, S., Pummer, E., Hrebrina, J., and Haeberli, W.: Causes, consequences and implications of the 2023 landslide-induced Lake Rasac glacial lake outburst flood (GLOF), Cordillera Huayhuash, Peru, Natural Hazards and Earth System Sciences, 25, 1207–1228, https://doi.org/10.5194/nhess-25-1207-2025, 2025.

Etzelmüller, B., Isaksen, K., Czekirda, J., Westermann, S., Hilbich, C., and Hauck, C.: Rapid warming and degradation of mountain permafrost in Norway and Iceland, The Cryosphere, 17, 5477–5497, https://doi.org/10.5194/tc-17-5477-2023, 2023.

Etzelmüller, B., Guglielmin, M., Hauck, C., Hilbich, C., Hoelzle, M., Isaksen, K., Noetzli, J., Oliva, M., and Ramos, M.: Twenty years of European mountain permafrost dynamics—the PACE legacy, Environmental Research Letters, 15, 104 070, https://doi.org/10.1088/1748-9326/abae9d, 2020.

Fan, X., Bhuyan, K., Wang, X., Cook, K. L., Ozturk, U., Loew, S., Gyamtsho, P., Jansen, J. D., and Xu, Q.: Rethinking policy on high mountain cascading hazards, Nature Geoscience, 18, 1066–1067, https://doi.org/10.1038/s41561-025-01834-w, 2025.

Fey, C., Wichmann, V., and Zangerl, C.: Influence of permafrost degradation and glacier retreat on recent high mountain rockfall distribution in the eastern European Alps, Earth Surface Processes and Landforms, 50, e70 063, https://doi.org/10.1002/esp.70063, 2025.

Fischer, L., Purves, R. S., Huggel, C., Noetzli, J., and Haeberli, W.: On the influence of topographic, geological and cryospheric factors on rock avalanches and rockfalls in high-mountain areas, Natural Hazards and Earth System Sciences, 12, 241–254, https://doi.org/10.5194/nhess-12-241-2012, 2012.

https://doi.org/10.5194/egusphere-2026-2821
Preprint. Discussion started: 6 July 2026

23460

Gruber, S.: Derivation and analysis of a high-resolution estimate of global permafrost zonation, The Cryosphere, 6, 221–233, https://doi.org/10.5194/tc-6-221-2012, 2012.

Gruber, S. and Haeberli, W.: Permafrost in steep bedrock slopes and its temperature-related destabilization following climate change, Journal of Geophysical Research: Earth Surface, 112, F02S18, https://doi.org/10.1029/2006JF000547, 2007.

Guardamino, L., Haeberli, W., Muñoz Asmat, R., Drenkhan, F., Tacsi, A., Cochachin, A., Colonia, D., Giraldez, C., Schauwecker, S., Torres Castillo, J., Braendle, E., and Frey, H.: Proyección de Lagunas Futuras en las Cordilleras Glaciares del Perú, Tech. rep., Lima, Peru, https://doi.org/10.13140/RG.2.2.27522.53442, 2019.

Haeberli, W. and Alean, J.: Temperature and Accumulation of High Altitude Firn in the Alps, Annals of Glaciology, 6, 161–163, https://doi.org/10.3189/1985AoG6-1-161-163, 1985.

Haeberli, W., Wegmann, M., and Vonder Mühll, D.: Slope stability problems related to glacier shrinkage and permafrost degradation in the Alps, Eclogae Geologicae Helvetiae, 90, 407–414, 1997.

Haeberli, W., Huggel, C., Kääb, A., Zgraggen-Oswald, S., Polkvoj, A., Galushkin, I., Zotikov, I., and Osokin, N.: The Kolka-Karmadon rock/ice slide of 20 September 2002: an extraordinary event of historical dimensions in North Ossetia, Russian Caucasus, Journal of Glaciology, 50, 533–546, https://doi.org/10.3189/172756504781829710, 2004.

Haeberli, W., Schaub, Y., and Huggel, C.: Increasing risks related to landslides from degrading permafrost into new lakes in de-glaciating mountain ranges, Geomorphology, 293, 405–417, https://doi.org/10.1016/j.geomorph.2016.02.009, 2017.

Harris, C., Arenson, L. U., Christiansen, H. H., Etzelmüller, B., Frauenfelder, R., Gruber, S., Haeberli, W., Hauck, C., Hölzle, M., Humlum, O., Isaksen, K., Kääb, A., Kern-L"utschg, M. A., Lehning, M., Matsuoka, N., Murton, J. B., Nötzli, J., Phillips, M., Ross, N., Seppälä, M., Springman, S. M., and Vonder Mühll, D.: Permafrost and climate in Europe: Monitoring and modelling thermal, geomorphological and geotechnical responses, Earth-Science Reviews, 92, 117–171, https://doi.org/10.1016/j.earscirev.2008.12.002, 2009.

Hartmeyer, I. and Otto, J.-C.: Rockfall, glacier recession, and permafrost degradation: long-term monitoring of climate change impacts at the Open-Air-Lab Kitzsteinhorn, Hohe Tauern, DEUQUA Special Publications, 5, 3–12, https://doi.org/10.5194/deuquasp-5-3-2024, 2024.

Hilbich, C., Hauck, C., Hoelzle, M., Scherler, M., Schudel, L., Völksch, I., Vonder Mühll, D., and Mäusbacher, R.: Monitoring mountain permafrost evolution using electrical resistivity tomography: A 7-year study of seasonal, annual, and long-term variations at Schilthorn, Swiss Alps, Journal of Geophysical Research: Earth Surface, 113, F01S90, https://doi.org/10.1029/2007JF000799, 2008.

Hilbich, C., Fuss, C., and Hauck, C.: Automated Time-lapse ERT for Improved Process Analysis and Monitoring of Frozen Ground, Permafrost and Periglacial Processes, 22, 306–319, https://doi.org/10.1002/ppp.732, 2011.

Jacquemart, M., Weber, S., Chiarle, M., Chmiel, M., Cicoira, A., Corona, C., Eckert, N., Gaume, J., Giacona, F., Hirschberg, J., Kaitna, R., Magnin, F., Mayer, S., Moos, C., van Herwijnen, A., and Stoffel, M.: Detecting the impact of climate change

https://doi.org/10.5194/egusphere-2026-2821
Preprint. Discussion started: 6 July 2026

on alpine mass movements in observational records from the European Alps, Earth-Science Reviews, 258, 104 886, https://doi.org/10.1016/j.earscirev.2024.104886, 2024.

Jacquemart, M., Brondex, J., Knuth, F., Weber, S., Kenner, R., Aaron, J., Gischig, V., de Silva, R., Spielmann, R., Schneider, M., Schumacher, D. I., Welty, E., Reist, F., Senn, I., and Farinotti, D.: Impact of permafrost changes on the 2025 Nesthorn-Birchgletscher hazard cascade, in: EGU General Assembly 2026, pp. EGU26–20 730, Vienna, Austria, https://doi.org/10.5194/egusphere-egu26-20730, 2026.

Keller, F.: Automated mapping of permafrost using the program PERMAKART within the Geographical Information System ARC/INFO, Permafrost and Periglacial Processes, 3, 133–138, 1992.

Kenner, R., Noetzli, J., Hoelzle, M., Raetzo, H., and Phillips, M.: Distinguishing ice-rich and ice-poor permafrost to map ground temperatures and ground ice occurrence in the Swiss Alps, The Cryosphere, 13, 1925–1941, https://doi.org/10.5194/tc-13-1925-2019, 2019.

Kenner, R., Arenson, L. U., and Grämiger, L.: Mass Movement Processes Related to Permafrost and Glaciation, in: Treatise on Geomorphology (Second Edition), edited by Shroder, J. J. F., pp. 283–303, Academic Press, Oxford, second edition edn., ISBN 978-0-12-818235-2, https://doi.org/10.1016/B978-0-12-818234-5.00112-7, 2022.

Kenner, R., Noetzli, J., Bazargan, M., and Scherrer, S. C.: Response of alpine ground temperatures to a rising atmospheric 0 °C isotherm in the period 1955–2021, Science of The Total Environment, 924, 171 446, https://doi.org/10.1016/j.scitotenv.2024.171446, 2024.

Kim, K. Y., Haagenson, R., Kansara, P., Rajaram, H., and Lakshmi, V.: Augmenting daily MODIS LST with AIRS surface temperature retrievals to estimate ground temperature and permafrost extent in High Mountain Asia, Remote Sensing of Environment, 305, 114 075, https://doi.org/10.1016/j.rse.2024.114075, 2024.

Koenig, C. E. M., Hilbich, C., Hauck, C., Arenson, L. U., and Wainstein, P.: Thermal state of permafrost in the Central Andes (27–34 S), The Cryosphere, 19, 2653–2676, https://doi.org/10.5194/tc-19-2653-2025, 2025.

Krautblatter, M. and Draebing, D.: Pseudo 3-D P-wave refraction seismic monitoring of permafrost in steep unstable bedrock, Journal of Geophysical Research: Earth Surface, 119, 287–299, https://doi.org/10.1002/2012JF002638, 2014.

Krautblatter, M. and Leith, K.: Glacier- and permafrost-related slope instabilities, in: The High-Mountain Cryosphere: Environmental Changes and Human Risks, pp. 147–165, Cambridge University Press, 2015.

Krautblatter, M., Verleysdonk, S., Flores-Orozco, A., and Kemna, A.: Temperature-calibrated imaging of seasonal changes in permafrost rock walls by quantitative electrical resistivity tomography, Journal of Geophysical Research: Earth Surface, 115, F02 003, https://doi.org/10.1029/2008JF001209, 2010.

Krautblatter, M., Huggel, C., Deline, P., and Hasler, A.: Research Perspectives on Unstable High-alpine Bedrock Permafrost: Measurement, Modelling and Process Understanding, Permafrost and Periglacial Processes, 23, 80–88, https://doi.org/10.1002/ppp.740, 2012.

Krautblatter, M., Funk, D., and Günzel, F. K.: Why permafrost rocks become unstable: a rock–ice-mechanical model in time and space, Earth Surface Processes and Landforms, 38, 876–887, https://doi.org/10.1002/esp.3374, 2013.

https://doi.org/10.5194/egusphere-2026-2821
Preprint. Discussion started: 6 July 2026

Kuhn, D., Hermanns, R. L., Fuchs, M., Schüßler, N., Torizin, J., Aga, J., Bendle, J., Eiken, T., and Balzer, D.: Warming-induced destabilization of polar coastal rock cliffs and the role of thermokarst: A case study of Forkastningsfjellet on Svalbard, Science of The Total Environment, 968, 178 807, https://doi.org/10.1016/j.scitotenv.2025.178807, 2025.

Kühni, A. and Pfiffner, O. A.: Drainage patterns and tectonic forcing: a model study for the Swiss Alps, Basin Research, 13, 169–197, https://doi.org/10.1046/j.1365-2117.2001.00146.x, 2001.

Magnin, F., Cathala, M., Bock, J., Ben-Asher, M., Josnin, J.-Y., Ravanel, L., and Deline, P.: Comprendre le rôle du permafrost dans la déstabilisation des versants rocheux de haute montagne. Bilan et perspectives de près de deux décennies d´étude dans les Alpes françaises, Rev. Fr. Geotech., p. 6, https://doi.org/10.1051/geotech/2026006, 2026.

Mamot, P., Weber, S., Schröder, T., and Krautblatter, M.: A temperature- and stress-controlled failure criterion for ice-filled permafrost rock joints, The Cryosphere, 12, 3333–3353, https://doi.org/10.5194/tc-12-3333-2018, 2018.

Mamot, P., Weber, S., Eppinger, S., and Krautblatter, M.: A temperature-dependent mechanical model to assess the stability of degrading permafrost rock slopes, Earth Surface Dynamics, 9, 1125–1151, https://doi.org/10.5194/esurf-9-1125-2021, 2021.

Margreth, S., Funk, M., Tobler, D., Dalban, P., Meier, L., and Lauper, J.: Analysis of the hazard caused by ice avalanches from the hanging glacier on the Eiger west face, Cold Regions Science and Technology, 144, 63–72, https://doi.org/10.1016/j.coldregions.2017.05.012, 2017.

Metzger, D.: A century of large rock slope failures in the European Alps: Influencing factors and climate change effects, Master's thesis, University of Zurich, Zurich, Switzerland, 2026.

Noetzli, J., Gruber, S., Kohl, T., Salzmann, N., and Haeberli, W.: Three-dimensional distribution and evolution of permafrost temperatures in idealized high-mountain topography, Journal of Geophysical Research: Earth Surface, 112, https://doi.org/10.1029/2006JF000545, 2007.

Noetzli, J., Isaksen, K., Barnett, J., Christiansen, H. H., Delaloye, R., Etzelmüller, B., Farinotti, D., Gallemann, T., Guglielmin, M., Hauck, C., Hilbich, C., Hoelzle, M., Lambiel, C., Magnin, F., Oliva, M., Paro, L., Pogliotti, P., Riedl, C., Schoeneich, P., Valt, M., Vieli, A., and Phillips, M.: Enhanced warming of European mountain permafrost in the early 21st century, Nature Communications, 15, 10 508, https://doi.org/10.1038/s41467-024-54831-9, 2024.

Nötzli, J. and Gruber, S.: Transient thermal effects in Alpine permafrost, The Cryosphere, 3, 85–99, https://doi.org/10.5194/tc-3-85-2009, 2009.

Obu, J., Westermann, S., Bartsch, A., Berdnikov, N., Christiansen, H. H., Dashtseren, A., Delaloye, R., Elberling, B., Etzelmüller, B., Kholodov, A., Khomutov, A., Kääb, A., Leibman, M. O., Lewkowicz, A. G., Panda, S. K., Romanovsky, V., Way, R. G., Westergaard-Nielsen, A., Wu, T., Yamkhin, J., and Zou, D.: Northern Hemisphere permafrost map based on TTOP modelling for 2000–2016 at 1 km2 scale, Earth-Science Reviews, 193, 299–316, https://doi.org/10.1016/j.earscirev.2019.04.023, 2019.

https://doi.org/10.5194/egusphere-2026-2821
Preprint. Discussion started: 6 July 2026

Offer, M., Weber, S., Krautblatter, M., Hartmeyer, I., and Keuschnig, M.: Pressurised water flow in fractured permafrost rocks revealed by borehole temperature, electrical resistivity tomography, and piezometric pressure, The Cryosphere, 19, 485–506, https://doi.org/10.5194/tc-19-485-2025, 2025.

Pandey, A. C., Islam, A., Dwivedi, C. S., Parida, B. R., Maslakov, A., and Koroleva, E.: Permafrost distribution modeling using remote sensing and machine learning technique in the Garhwal Himalaya, India, Environmental Earth Sciences, 85, 35, 2025.

Pfluger, F., Weber, S., Steinhauser, J., Zangerl, C., Fey, C., Fürst, J., and Krautblatter, M.: Massive permafrost rock slide under a warming polythermal glacier deciphered through mechanical modeling (Bliggspitze, Austria), Earth Surface Dynamics, 13, 41–70, https://doi.org/10.5194/esurf-13-41-2025, 2025.

Råback, P., Malinen, M., Ruokolainen, J., and CSC – IT Center for Science: Elmer Solver Manual, CSC – IT Center for Science, Espoo, Finland, 2020.

Ravanel, L. and Deline, P.: Climate influence on rockfalls in high-Alpine steep rockwalls: The north side of the Aiguilles de Chamonix (Mont Blanc massif) since the end of the Little Ice Age, The Holocene, 21, 357–365, https://doi.org/10.1177/0959683610374887, 2011.

Ravanel, L., Guillet, G., Kaushik, S., Preunkert, S., Malet, E., Magnin, F., Trouvé, E., Montagnat, M., Yan, Y., and Deline, P.: Ice aprons on steep high-alpine slopes: insights from the Mont-Blanc massif, Western Alps, Journal of Glaciology, 69, 1275–1291, https://doi.org/10.1017/jog.2023.15, 2023.

Sattar, A., Allen, S., Mergili, M., Haeberli, W., Frey, H., Kulkarni, A. V., Haritashya, U. K., Huggel, C., Goswami, A., and Ramsankaran, R. A. A. J.: Modeling potential glacial lake outburst flood process chains and effects from artificial lake-Level lowering at Gepang Gath Lake, Indian Himalaya, Journal of Geophysical Research: Earth Surface, 128, e2022JF006 826, https://doi.org/10.1029/2022JF006826, 2023.

Sattar, A., Cook, K. L., Rai, S. K., Berthier, E., Allen, S., Rinzin, S., de Vries, M. V. W., Haeberli, W., Kushwaha, P., Shugar, D. H., Emmer, A., Haritashya, U. K., Frey, H., Rao, P., Gurudin, K. S. K., Rai, P., Rajak, R., Hossain, F., Huggel, C., Mergili, M., Azam, M. F., Gascoin, S., Carrivick, J. L., Bell, L. E., Ranjan, R. K., Rashid, I., Kulkarni, A. V., Petley, D., Schwanghart, W., Watson, C. S., Islam, N., Gupta, M. D., Lane, S. N., and Bhat, S. Y.: The Sikkim flood of October 2023: Drivers, causes, and impacts of a multihazard cascade, Science, 387, eads2659, https://doi.org/10.1126/science.ads2659, 2025.

Scandroglio, R., Draebing, D., Offer, M., and Krautblatter, M.: 4D quantification of alpine permafrost degradation in steep rock walls using a laboratory-calibrated electrical resistivity tomography approach, Near Surface Geophysics, 19, 241–260, https://doi.org/10.1002/nsg.12149, 2021.

Shugar, D. H., Jacquemart, M., Shean, D., Bhushan, S., Upadhyay, K., Sattar, A., Schwanghart, W., McBride, S. K., Van Wyk de Vries, M., Mergili, M., Emmer, A., Deschamps-Berger, C., McDonnell, M., Bhambri, R., Allen, S., Berthier, E., Carrivick, J., Clague, J. J., Dokukin, M., Dunning, S., Frey, H., Gascoin, S., Haritashya, U., Huggel, C., Kääb, A., Kargel, J., Kavanaugh, J., Lacroix, P., Petley, D., Rupper, S., Azam, M. F., Cook, S., Dimri, A. P., Eriksson, M., Farinotti, D., Fiddes,

https://doi.org/10.5194/egusphere-2026-2821
Preprint. Discussion started: 6 July 2026

J., Gnyawali, K., Harrison, S., Jha, M., Koppes, M., Kumar, S., Leith, K., Majeed, U., Mal, S., Muhuri, A., Nötzli, J., Paul, F., Rashid, I., Sain, K., Steiner, J., Ugalde, F., Watson, C. S., and Westoby, M.: A massive rock and ice avalanche caused the 2021 disaster at Chamoli, Indian Himalaya, Science, 373, 300–306, https://doi.org/10.1126/science.abh4455, 2021.

Stewart-Jones, E. and Gruber, S.: Transferring cryosphere knowledge between mountains globally: A case study of western Canadian mountains, the European Alps and the Scandes, Journal of Alpine Research, Revue de géographie alpine, 2023.

Stoffel, M., Trappmann, D., Corona, C., et al.: Rockfall from an increasingly unstable mountain slope driven by climate warming, Nature Geoscience, 17, 249–254, https://doi.org/10.1038/s41561-024-01390-9, 2024.

Suter, S., Laternser, M., Haeberli, W., Frauenfelder, R., and Hoelzle, M.: Cold firn and ice of high-altitude glaciers in the Alps: measurements and distribution modelling, Journal of Glaciology, 47, 85–96, https://doi.org/10.3189/172756501781832566, 2001.

Walter, F., Amann, F., Kos, A., Kenner, R., Phillips, M., de Preux, A., Huss, M., Tognacca, C., Clinton, J., Diehl, T., and Bonanomi, Y.: Direct observations of a three million cubic meter rock-slope collapse with almost immediate initiation of ensuing debris flows, Geomorphology, 351, 106 933, https://doi.org/10.1016/j.geomorph.2019.106933, 2020.

Weber, S., Vieli, A., Phillips, M., and Cicoira, A.: Thermal diffusivity of mountain permafrost derived from borehole temperature data in the Swiss Alps, The Cryosphere, 19, 6727–6748, https://doi.org/10.5194/tc-19-6727-2025, 2025.

Wegmann, M., Gudmundsson, G. H., and Haeberli, W.: Permafrost changes in rock walls and the retreat of alpine glaciers: a thermal modelling approach, Permafrost and Periglacial Processes, 9, 23–33, https://doi.org/10.1002/(SICI)1099-1530(199801/03)9:1<23::AID-PPP274>3.0.CO;2-Y, 1998.

Yang, H., Tang, J., Chang, X., Wang, J., Gong, W., Wang, D., and Xing, Y.: Permafrost degradation: A critical driver of aboveground carbon sink loss in China's boreal forests, Catena, 265, 109 912, https://doi.org/10.1016/j.catena.2026.109912, 2026.